When motion appears stopped: Stereo motion standstill

Chia-huei Tseng, Joetta L. Gobell, Zhong-Lin Lu, and George Sperling

PNAS 2006;103;14953-14958; originally published online Sep 26, 2006;
doi:10.1073/pnas.0606758103

When motion appears stopped: Stereo motion standstill

Chia-huei Tseng*[†‡], Joetta L. Gobell*, Zhong-Lin Lu[§], and George Sperling*[‡¶]

Departments of *Cognitive Sciences and [¶]Neurobiology and Behavior and Institute of Mathematical Behavioral Sciences, University of California, Irvine, CA 92697; and [§]Laboratory of Brain Processes, Department of Psychology, University of Southern California, Los Angeles, CA 90089

Contributed by George Sperling, August 9, 2006

Motion standstill is different from the usual perceptual experiences associated with objects in motion. In motion standstill, a pattern that is moving quite rapidly is perceived as being motionless, and yet its details are not blurred but clearly visible. We revisited motion standstill in dynamic random-dot stereograms similar to those first used by Julesz and Payne [Julesz B, Payne R (1968) *Vision Res* 8:433–444]. Three improvements were made to their paradigm to avoid possible confounds: The temporal frequency of the motion stimuli was manipulated independently from that of individual stereo gratings so that the failure of motion perception is not due to inability to compute stereo. The motion of the stereo gratings was continuous across the visual field so that the perceived pattern in motion standstill was not a simple average of a back-and-forth display wobble over time. Observers discriminated three spatial frequencies to demonstrate pattern recognition. Three objective psychophysical methods, instead of merely self-report, were used to objectively demonstrate motion standstill. Our results confirm that motion standstill occurs in dynamic random-dot stereogram motion displays at 4–6 Hz. Motion standstill occurs when the stimulus spatiotemporal frequency combination exceeds that of the salience-based third-order motion system in a spatiotemporal frequency range in which the shape and depth systems still function. The ability of shape systems to extract a representative image from a series of moving samples is a significant component of a biological system's ability to derive a stable perceptual world from a constantly changing visual environment.

illusions | perception | psychophysics | stereopsis | vision

There are several categories of perceptual experience associated with objects in motion. When an object moves very slowly, such as the moon moving across the night sky, we are not aware of the motion even though we can clearly see the object. As the speed of an object increases, we begin to perceive motion. When we see a strolling cat, a child riding a bicycle, or a leaf blowing in the wind, we recognize the object while also having a clear sense of its motion. Beyond a certain speed, objects become blurred, but we still can perceive their motion, as occurs when riding in a train and a second train passes in the opposite direction on an adjacent track.

A class of phenomena termed "motion standstill," distinct from the perceptual experiences mentioned above, provides valuable information about the limits of both human motion and pattern computations. In motion standstill, an observer perceives a pattern that is moving quite rapidly as being motionless while its details are clearly visible. This study is concerned with a particular motion standstill phenomenon, stereo motion standstill. The percept of the stereo motion studied here is computed by the "third-order" motion system, so this is an instance of third-order motion standstill. An overview of motion standstill is given below, followed by a detailed investigation of stereo motion standstill.

Motion Standstill Phenomena. ***The significance of motion standstill.*** The significance of motion standstill is that it demonstrates that the pattern-recognition system can produce a single, stable perceptual image from a changing sequence of images that represent movement. This principle as a goal of human pattern recognition was clearly enunciated by Lu *et al.* (1, 2). They also proposed a theory for the circumstances under which the (third-order) motion system would fail but pattern recognition might easily succeed and thereby produce the phenomenon of motion standstill. Earlier reports had concentrated on motion standstill as a failure of motion perception, which of course it is. However, failure of motion perception in itself is an incomplete account of the phenomenon. Motion perception must fail, yes, but concurrently, pattern recognition must succeed. That a sequence of rapidly translating images can provide the perception of a stable, motionless object is the remarkable aspect of the phenomenon of motion standstill.

Parameters of motion standstill. Motion standstill has been observed in isoluminant color motion (1–8), stroboscopic motion (9–15), motion adaptation (16–20), and stereo motion (21). The temporal frequency range in which motion standstill is most frequently reported is <6 Hz, well within the range in which motion is easily detected. This range indicates that the failure of an observer to detect motion (both the direction and velocity) is not simply due to the stimulus exceeding temporal resolution of the human visual motion system. Rather, motion detection fails because, for various other reasons, input to the motion system is too weak to enable a motion computation. Motion standstill in the displays mentioned above occurred over a wide selection of sizes, contrasts, and spatial arrangements, as well as at both fovea and periphery. One important shared attribute, which is also the critical feature that sets motion standstill apart from the blur of extremely fast-moving objects, is the observer's ability to identify spatial details in the moving stimulus. Observers sometimes find that the moving patterns gradually fade if they remain fixated after the motion standstill phenomenon begins. This fading is similar to the Troxler effect, in which a stationary stimulus in the periphery disappears after prolonged gaze (22).

Stereo Motion Standstill Phenomena. ***Binocular standstill.*** Julesz and Payne (21) reported motion standstill in stereoscopic displays using dynamic random-dot stereograms (DRDSs). They used 100×100 black and white random dots to portray a binocularly defined grid moving back-and-forth between two spatial locations or tilting back-and-forth $\pm 6°$. In one of their main conditions, a stereogram depicted a 0.95 cycles per degree (c/d) vertical grid composed of eight thick lines raised forward in depth on a flat surface. This grid alternated between two adjacent positions separated by 120° of the grid period, equivalent to 0.35° of visual angle. At slow alternation rates, back-and-forth motion was perceived. At high alternation rates (>8–10 Hz), observers perceived wide horizontal bars in the frontal plane (simultaneity) but no motion. Wide bars are what

Author contributions: C.-h.T., J.L.G., Z.-L.L., and G.S. designed research, performed research, analyzed data, and wrote the paper.

The authors declare no conflict of interest.

Abbreviations: DRDS, dynamic random-dot stereogram; c/d, cycles per degree.

[†]Present address: Institute of Cognitive Science, National Cheng Kung University, No. 1, University Road, Tainan City 701, Taiwan, Republic of China.

[‡]To whom correspondence may be addressed. CH_Tseng@alumni.uci.edu and sperling@uci.edu.

would be expected from algebraic summation of the component stimuli. At ≈4–7 Hz, motionless bars of normal width were perceived in the frontal plane location (i.e., only one intermediate position of the laterally back-and-forth moving grid was perceived). The authors called this phenomenon binocular standstill. It was noted that to experience strong binocular standstill, the random-dot textures in successive frames must be uncorrelated. Correlated textures in successive frames produced a strong monocular motion cue, and observers did not experience standstill with this stimulus.

Three possible confounds in the stimuli of Julesz and Payne (1968). The display used by Julesz and Payne raises three concerns about the validity of their observations. (*i*) Back-and-forth motion represents a minimal stimulation of a motion system; the two opposite motion directions might tend to cancel each other. A much stronger test for the failure of the whole motion system would be the perception of standstill during continuous motion in one direction. (*ii*) In both classes of Julesz and Payne's stimulus movement (translation or rotation) and for both of their stimulus configurations, the successive frames alternated between two strongly overlapping locations. When standstill was reported, the object was perceived as static in the center of the display. This percept is very similar to the spatial average of the two image frames. In a stronger test, the spatial average of frames would be very different from the standstill percept. (*iii*) The spatial-alternation frequency was confounded with the frame rate of new dynamic stereograms. At high alternation frequencies (e.g., 10 Hz), each stereogram is displayed for a shorter period (100 ms per spatial location) than at slow alternation frequencies (200 ms per spatial location at 5 Hz). This procedure will produce weaker stereo inputs at high alternation frequencies than at low alternation frequencies. Weakening of the stereo cues was thereby confounded with a weakening of the motion cue. Perhaps because of these three problems, Julesz and Payne's claim of stereo motion standstill was overlooked or ignored for 31 years until Lu *et al.* (2) demonstrated motion standstill in isoluminant chromatic displays. Indeed, the deficiencies in the study by Julesz and Payne motivated us to reexamine binocular standstill with a better-controlled paradigm to determine whether it actually occurs.

Improvements in the current study. Unidirectional movement. To address the concern that binocular standstill may be a net result of the minimal motion stimulation produced by rapidly alternating motion in two opposite directions, the stimuli used here contained only one moving direction. On each trial, five frames of DRDSs depicted depth-gratings that translated vertically from frame-to-frame, either up or down (Fig. 1), providing multiple frames on each trial rather than the two provided by the stroboscopic back-and-forth motion.

Clearly differentiating the standstill percept from the average of the motion frames. We use displays consisting of five frames translating in the same direction. Spatial averages of depths generated by this display are completely different from the depth in any single frame (the standstill perception), unlike back-and-forth motion between overlapping frames.

Constant stereo-frame rate. To provide equal stereo inputs at different temporal frequencies of motion, the displays were designed to produce a new random-dot stereogram at a constant rate (every 50 ms for observers AN and CT and 67.7 ms for observer YT). The duration of each DRDS reflected the minimum time requirement for an individual subject to fuse and generate reliable stereo images. The rate of new stereo frames was independent of the temporal frequency of the motion stimuli (which is determined by the number of stimulus wavelengths moved per second). This design ensures that the quality of the stereo input is not confounded with motion frequency, which is critical when evaluating the failure of a motion system. With this design, failure of motion perception with an increase in motion temporal frequency can be attributed to limitations of the motion systems and not to limitations in stereopsis.

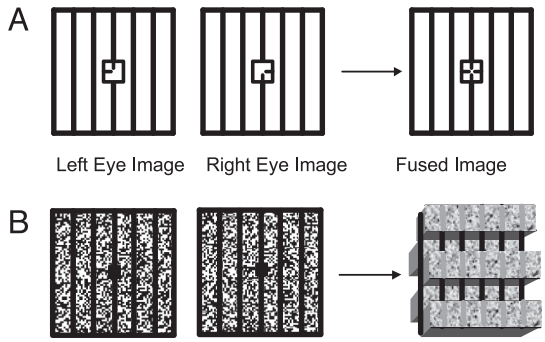

Fig. 1. Stimulus configuration. (*A*) The fixation frame for all experiments. The black vertical lines and central square were displayed before each trial and continued throughout the trial to help observers maintain vergence on an intermediate depth plane (the horopter) exactly between the front and rear depth planes of the moving random-dot stereograting. Each trial began with display of a Nonius consisting of an incomplete cross in each eye that became a complete cross only upon correct binocular vergence and binocular fusion. Upon fusion, the observer pressed a key that caused the Nonius to disappear and stimulus motion to begin immediately. (*B*) A sample pair of left-eye and right-eye frames of a dynamic random-dot stimulus. Stereoscopically fusing the left- and right-eye images produces a binocular ''fused image'' of four horizontal bars alternating between two depth planes illustrated partially and schematically in the lower right image. The vertical lines appear transparently behind the horizontal bars. The sequence of frames defines a horizontal squarewave depth-grating moving up or down. Each successive pair of frames is independently constructed (only the left–right eye correlation pattern translates), so there is no monocular cue to motion or pattern.

Temporally uncorrelated random-dot texture. In all of the experiments, the motion displays consisted of stereoscopically defined horizontal squarewave gratings composed of DRDSs. Each DRDS had left and right images that were correlated (and portrayed a binocular grating). The random-dot texture in successive DRDSs was uncorrelated to ensure that no luminance or texture information was available for motion computation.

Observer tasks. Three tasks were used to provide an objective and quantitative evaluation of stereo motion standstill. The three tasks were administered in three separate experiments as follows: direction discrimination, pattern recognition, and speed rating. Motion standstill implies (*i*) that observers were unable to discriminate the direction of motion, (*ii*) that the display appeared motionless, and (*iii*) that the observers could report details of the stimuli as if they were physically standing still, in this case, the spatial frequency of the stereoscopic bars.

Results

Experiment 1: Motion-Direction Discrimination. Three observers judged the motion direction of stereo squarewave gratings defined by DRDSs. Accuracy of direction discrimination (expressed as a percentage, P_{obs}) is corrected for guessing (P_{guess}) as follows: The observed accuracy (P_{obs}) is assumed to be the sum of two kinds of events: the proportion of trials on which the observer correctly perceives the direction (true accuracy, P_{true}) and the other trials on which the observer fails to perceive the direction and guesses correctly. The guessing rate (P_{guess}) in this experiment is 50% (only two possible responses in each trial). These assumptions imply Eq. **1**:

$$P_{obs} = P_{true} + (1 - P_{true})P_{guess}. \quad [1]$$

At perfect performance, $P_{obs} = 100\%$ and $P_{true} = 100\%$. At chance performance, $P_{obs} = 50\%$ and $P_{true} = 0$.

Fig. 2 shows guess-corrected accuracy P_{true} as a function of temporal frequency (open circles). P_{true} for all observers declined with increasing temporal frequency. In seven of nine cases, P_{true} declined to ≤50% as the temporal frequency of the motion stimulus

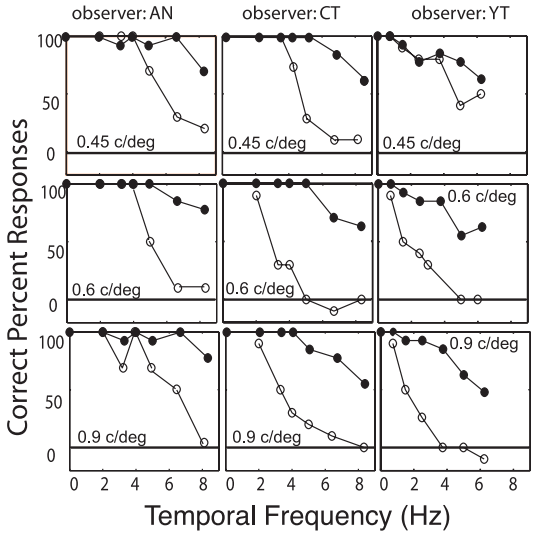

Fig. 2. Guessing-corrected accuracy of direction discrimination (open circles) and of pattern discrimination (filled circles) as a function of the temporal frequency of vertically translating stereo gratings: results from three observers. On direction-discrimination trials, observers judged the motion direction (up, down) of the horizontal stereo depth-gratings; on pattern-discrimination trials, observers discriminated the spatial frequency of the moving stereo gratings (thin, medium, or thick stripes). Feedback was provided. The solid line at 0 represents chance performance.

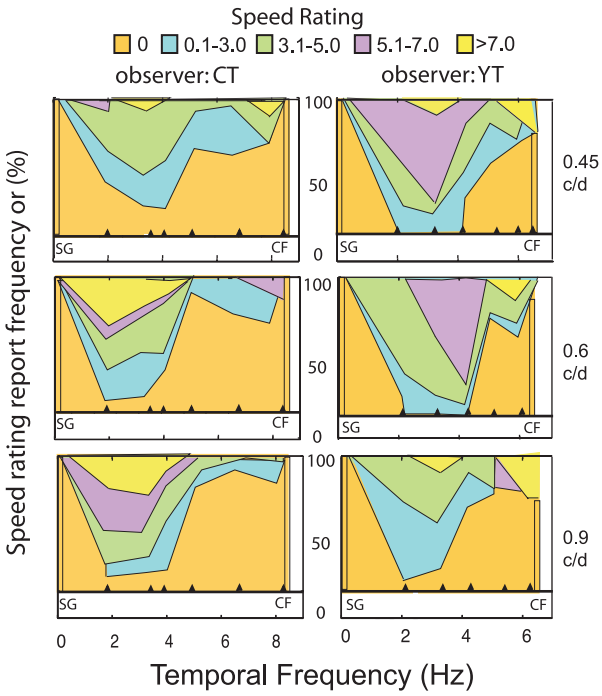

Fig. 3. The distribution of speed ratings as a function of temporal frequency of vertically translating stereo gratings. Objective speed is temporal frequency divided by spatial frequency. Observers rated the perceived speed of motion on a previously trained numeric scale (0–10), with 0 indicating stationary and 10 indicating the fastest motion. Ratings are grouped into five categories represented by distinctive colors: orange, 0 (stationary); yellow, ratings of >7. Purple, blue, and green represent intermediate speed ratings from 0.1 to 6.9. Each panel shows the frequency of the speed rating categories (*y* axis) for all tested temporal frequencies (*x* axis) for a particular observer and spatial frequency. Two embedded control conditions displayed objectively stationary gratings: a physically static grating (SG) (temporal frequency = 0) and a counterphase flickering grating (CF) (temporal frequency as indicated).

increased from 1 to 5 Hz and approached 0% beyond 6 Hz. Notably, observers reported that they were occasionally unable to determine motion direction because the horizontal bars did not seem to move. Observer performance in this task defines a region in which motion perception is impaired. However, the failure to discriminate motion direction could be due to a failure of the depth/shape system, to failure of the motion systems, or to some combination of the two. Experiment 2 investigated shape perception.

Experiment 2: Pattern Recognition. The same observers viewed identical stimuli as in Experiment 1. In Experiment 2, observers were required to report the perceived spatial pattern (thin, medium, or thick) of the moving stereo gratings. The procedure to correct for guessing is the same as in Experiment 1, except the guessing rate (P_{guess}) here is 33% (three possible responses). Guessing-corrected accuracy (P_{true}) is plotted as a function of temporal frequency in Fig. 2.

Although pattern-discrimination accuracy declined as the motion frequency increased, the decline occurred at higher temporal frequencies (>6 Hz) than those at which motion-direction discrimination declined in Experiment 1 (≈4 Hz). Also, the decline was more gradual than the decline in motion-direction discrimination. At all tested temporal frequencies (0–8.3 Hz), the accuracy for pattern discrimination was well above chance. At temporal frequencies at which observers could not determine the direction of movement in Experiment 1, they were nevertheless able to accurately report the spatial frequency of the moving patterns in Experiment 2.

Experiment 3: Speed Rating. Experiments 1 and 2 showed that there were spatial and temporal frequency combinations in which observers were able to perceive the spatial structure of a moving stimulus but unable to perceive its direction of motion. Observers reported that the horizontal squarewave gratings were stable at a location, whereas the random-dot texture continued to change dynamically. Occasionally, the horizontal gratings appeared to jump just once (from one position to another) during the five-frame presentation. These observations suggested that motion standstill did occur. In Experiment 3, we offered observers the opportunity to give a precise numeric estimate between 0 (stationary) and 10 (maximum speed) of the perceived stimulus speed based on a trained scale. Two observers (CT and YT) participated in this experiment, and both of them assigned perfect speed ratings when retested with training stimuli embedded in the main experiment.

Observers' responses are tabulated in five categories based on the rated numbers: (*i*) 0 rating, (*ii*) rating between 0.1 and 3, (*iii*) rating between 3.1 and 5, (*iv*) rating between 5.1 and 7, and (*v*) rating between 7.1 and 10. Fig. 3 summarizes observers' speed ratings for all spatial and temporal frequencies.

Control conditions. There were two kinds of objectively nonmoving stimuli: the stationary grating and the counterphase flickering grating (8.3 Hz for observer CT; 6.3 Hz for observer YT). Both were always rated as zero speed by observer CT at all three tested spatial frequencies. Observer YT also always rated the stationary grating as 0 but occasionally rated the counterphase grating as 10 (maximum speed) when, according to his subsequent report, he was unable to judge its direction and therefore assumed it must have been moving too fast.

Frequency of speed ratings of zero. Grating speed is equal to temporal frequency divided by spatial frequency. As speed increases from 2 Hz (the lowest tested temporal frequency), Fig. 3 shows that both the rated speed and the frequency of zero-speed ratings increased. At >5 Hz, however, >50% of trials produced speed ratings of zero.

Discussion

Theoretical Conditions for Motion Standstill. We have three criteria for the perception of motion standstill in a moving stimulus: A

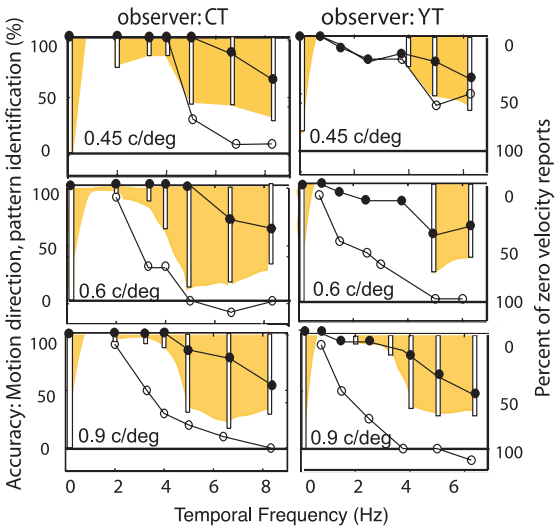

Fig. 4. Accuracy of motion-direction discrimination, accuracy of pattern identification, and percentage of zero-motion (stationary) judgments as a function of temporal frequency. Data are from two observers (CT and YT) who participated in all three tasks (motion-direction discrimination, pattern recognition, and speed rating). Observers' guessing-corrected accuracy of motion direction (open circles) and pattern recognition (filled circles) and the frequency of report of "speed equals zero" (vertical bars) are plotted as a function of temporal frequency (in hertz) for three different spatial frequencies as indicated in the panels. The high frequency of zero-motion reports combined with almost zero accuracy of motion-direction discrimination combined with very high accuracy of pattern recognition confirm that perceptual motion standstill occurred with high likelihood for moving stereo gratings presented at temporal frequencies of >4–5 Hz.

speed rating of zero, the inability to determine motion direction, and nevertheless the ability to see details of the stimulus as when it is objectively standing still. These three elements are brought together in Fig. 4.

Empirical Proof of Motion Standstill. The area between the upper curve (pattern discrimination) and lower curve (motion discrimination) represents trials on which a pattern was perceived but motion-direction discrimination failed. The orange area represents the percentage of trials on which speed was judged as zero. The intersection of these two areas satisfies the three conditions for motion standstill. Fig. 4 shows that for the two higher spatial frequencies (0.6 and 0.9 c/d) at temporal frequencies of >5 Hz, the majority of trials, but not quite all trials, satisfy the conditions of motion standstill (i.e., there is trial-to-trial variability).

Standstill in Continuous Movement Versus Back-and-Forth Wobble. The problem with Julesz and Payne's back-and-forth wobbling display (21) is that the percept of motion standstill is so suspiciously similar to the average of the two alternating displays that standstill is not convincingly demonstrated. That a grating that moves continuously in one direction can appear to be standing still with clearly visible details is more remarkable. This improvement to Julesz and Payne's procedure makes it clear that motion standstill in stereoscopic displays is not a result of simple averaging over successive displays, and it validates their original observations.

Motion Standstill Implies That Pattern Perception Processes Succeed in Extracting Shape from Moving Patterns. How? The phenomenon of motion standstill in our stimuli implies that pattern information can be extracted by visual shape-recognition systems from rapidly moving displays at temporal and spatial frequencies beyond the resolution of the third-order motion system.

Lu *et al.* (2) distinguished two mechanisms by which the pattern/shape system might extract the standstill shape from the moving stimulus: a snapshot model in which a brief instance in time is sampled, or more likely, a translation-invariant shape computation (e.g., ref. 23) as was originally proposed for V1 complex cells by Hubel and Wiesel (24). Ecologically, there is good reason for a translation-resistant shape-recognition system to have evolved. In normal viewing, especially during walking or running, random sweeps of images on the retina are large in relation to shape details that would be useful and that are, in fact, easily perceived (25).

The Phenomenal Appearance of Motion Standstill. The standstill perception of Lu *et al.*'s (2) translating red–green grating was exactly that of a stationary grating. Because the grating was both isoluminant and isosalient, the first- and third-order motion systems were not stimulated, and standstill could occur at any (even quite low) spatial and temporal frequencies (2), well within the resolution of the color/shape/pattern systems. In contrast, first- and second-order motion standstill can be best observed in very-high-spatial-frequency gratings in a range of temporal frequencies.‖ If one looks at a display of such a translating luminance grating (first-order) or a texture contrast-modulated grating (second-order) from a large distance, neither the grating nor its motion are visible. As one approaches, there is a narrow range of distances at which a grating becomes visible but not its motion (i.e., motion standstill). Still closer, both the grating and its motion are clearly resolved. The perception of a barely resolvable, very-high-spatial-frequency grating in motion standstill is somewhat flickery, different from the rock-solid stability of standstill in the isoluminant, isosalient, red–green low-spatial-frequency grating. The standstill appearance of the DRDS depth-gratings has a similar flickery aspect. These last three cases of motion standstill (first-order, second-order, and DRDS stereo) occur within the narrow spatiotemporal frequency range between failure of motion and failure of shape/pattern perceptual computations.

Our translating gratings occupied five different positions (only four positions when the frame-to-frame shift was 90°). On trials in which standstill was experienced, the phenomenal experience in both stereo and color grating experiments was of a grating in only one representative position. Informal observations of the perceived position of the standstill stereo depth-gratings suggest that grating position is distributed among all of the presented positions; it is not invariably the first or last or any particular intermediate position. Our current study does not directly answer which frame of a multiframe display best represents motion standstill; there seems to be both individual and trial-to-trial variability. A more extensive study is required to address this question.

Stereo Motion Is Third-Order Motion. In the three-motion-systems theory proposed by Lu and Sperling (26), the first-order motion system computes the motion of areas defined by luminance (or more accurately, by similar V1 simple cells), and the second-order motion system computes the motion of areas defined by the amount of texture contrast (i.e., luminance variance). In our stereoscopic displays, the moving grating was defined neither by luminance nor by texture, so both the grating and its motion were invisible to the first- and second-order motion systems. The third-order motion system computes motion from areas defined by their salience (e.g., from figure–ground relationships, no matter how figure–ground is determined). In the case of stereo-defined gratings, the foreground bars typically are perceived as "figure," and the background bars are the "ground."

‖Sperling, G., Lyu, S., Kim, H. (2002) *J. Vision* 2(7):256a (abstr.).

There is compelling evidence that stereo motion is processed solely by the third-order motion system (27, 28). The main arguments involve the temporal cutoff/corner frequency, alternating feature displays, the documented failure of alternative explanations, and the fact that two different motions (isoluminant and stereo) in the same direction can nevertheless cancel each other if they are out of phase (29).** More specifically: (*i*) Whereas the corner frequency for first- and second-order motions is 10–12 Hz, stereo motion falls off at the same corner frequency (≈4 Hz) as other third-order motions. (*ii*) Stereo motion fails the pedestal test (i.e., observers are unable to perceive the motion of a moving sinewave added to a stationary sinewave with twice the amplitude, whereas first- and second-order motion are unaffected). (*iii*) Replacing every other frame of a stereo-defined grating motion stimulus with a frame in which the grating is defined instead by contrast (i.e., a dark–light grating) leaves the perception of motion intact, except that the direction now depends (as predicted) on whether the observer perceives the dark or light bars as figure (30). It is highly implausible that evolution would have developed specialized mechanisms to correlate all of the feature pairs that successfully produce alternating feature motion. A single mapping of features into salience is the obvious mechanism. (*iv*) The failure of experiments that seek to demonstrate specialized stereo motion mechanisms is documented in ref. 27. (*v*) Consider an isoluminant red–green grating in which the red and green stripes are faintly saturated, just enough to enable ≈80% accuracy in motion-direction discrimination when the grating moves up or down. Also consider a dynamic random-dot stereograting, such as those used in the present experiments, moving at a temporal frequency for which motion-direction discrimination also is 80% correct. If these gratings have the same temporal and spatial frequency, then there is a phase and a degree of saturation of the colors of the isoluminant grating such that when these two gratings are added together, the perception of motion is cancelled (29).** For example, when the observer perceives the foreground grating as figure and the red bars of the red–green grating as figure, adding red to the background makes the background just as salient as the foreground, so there is no salience modulation and, therefore, no third-order motion. Adding the two gratings in the opposite phase (i.e., adding red to the foreground) improves motion-direction discrimination. This kind of phase dependency (cancellation or enhancement) is proof that the motion computation for both gratings occurs within the same mechanism, which in this case is the mechanism that has been called third-order motion perception.

Stereo Motion Standstill Is Easy to Produce. Until recently, motion standstill has been observed very infrequently because the circumstances for observing it have not been fully understood. Motion standstill does not merely involve a failure of the motion system; it also requires success of shape, pattern, and/or color systems. The first-order and second-order motion systems have extremely good temporal resolution. The only chance of finding stimuli that might produce standstill is at the limits of spatial resolution, which is slightly better in the shape/texture systems than in the corresponding motion systems. First- and second-order motion standstill can be observed by producing a high-spatial-frequency moving grating and backing away from it until a point is reached where the grating is still visible but the direction of motion has become indeterminate and it no longer appears to be moving, just before the grating itself becomes invisible.

The temporal resolution of the third-order motion system is only one-third that of the first- and second-order motion system, so there is potentially a wide range of temporal frequencies where motion fails before shape/texture/color. The difficulty in demonstrating isoluminant color motion is that the visual system is so extraordinarily sensitive to luminance that slight statistical inhomogeneities in color sensitivity produce luminance-motion artifacts. Other third-order motion stimuli typically rely on attention (e.g., motion-from-motion and most alternating feature displays) and do not have a strong automatic bottom-up saliency component. Because depth-defined motion in dynamic random-dot displays does not stimulate first- or second-order motion systems, any motion that is perceived is third-order motion. Unfortunately, acuity for stereo depth-gratings is not nearly as good as acuity for luminance gratings, so the potential range for motion standstill is not as great as might be expected. Nevertheless, to date, all stereo-normal observers have been able to perceive the motion of depth-defined areas in DRDSs, and thereby perceive "guaranteed" pure third-order motion, and therefore to perceive motion standstill. With many ways to present separate stimuli to the two eyes, such as red–blue anaglyphs, random-dot stereo motion is perhaps the simplest pure third-order motion to demonstrate motion standstill. Most natural stimuli involve at least two and often all three motion systems, so the problem is not producing third-order motion but producing pure third-order motion. Stereo motion generated from DRDSs is intrinsically free of luminance contamination and thus bypasses the extensive calibration (2) required to produce most other pure third-order motion stimuli.

Summary and Conclusions. Motion standstill can be observed in stimuli for which the resolution of shape/texture/color systems exceeds that of the combined motion systems. We obtained reliable percepts of motion standstill by manipulating the spatial–temporal frequencies of DRDSs in which a horizontal depth-defined grating moved continuously either upward or downward. Motion standstill occurred with high probability at temporal frequencies of 4–6 Hz, in conditions in which details of the stimulus such as the thickness and number of stripes were clearly visible. Thus, by inactivating the motion systems, the stereo depth system is shown to deliver to conscious perception a single representative view of the rapidly moving stimulus.

Methods

Stimulus Parameters. The motion stimuli subtended 6.7 × 6.7° and consisted of images made of 144 × 144 black-and-white picture elements (pixels) whose polarity (black or white) was selected at random. Horizontal stripes of 24, 18, and 12 picture elements wide (vertically) produced squarewave gratings with spatial frequencies of 0.45, 0.6, and 0.9 c/d, respectively, at a viewing distance of 68 cm. Temporal frequencies ranged from 0.75 to 8.33 Hz, generated by varying the amount of phase shift between consecutive frames.

Horopter Defined and Controlled. The stimuli were viewed stereoscopically to provide the perception of horizontal stripes that alternated between two depth planes, one behind the horopter and the other in front. It is critical to situate the horopter precisely between the two depths of the stereo image to avoid possible rivalry motion, which also provides inputs to the third-order motion system and is almost as strong as stereo motion.†† To control vergence, thick black vertical lines in the plane of the horopter were superimposed on the random-dot images (Fig. 1*A*) and remained present throughout the trial. These lines define the horopter, and fusing them binds vergence to the horopter. The stereo depth-grating was produced by creating left and right images that were identical except for horizontal shifts.

**Tseng, C. H., Gobell, J., Sperling, G. (2004) *Perception* 33(Suppl.):154 (abstr.).

††Kim, H. J., Lu, Z.-L., Sperling, G. (2001) *Invest. Ophthalmol. Visual Sci. ARVO J.* Suppl. 42:3947 (abstr).

In the example in Fig. 1*B*, the odd horizontal bars of the right image are shifted to the left, and the even bars are shifted to the right. When viewed monocularly, left and right images gave the impression of an entirely random dynamic texture. As a result of the binocular disparity, when the left and right images were stereoscopically fused, the binocular perception was of alternating stripes at different depths.

Apparatus. All motion displays were shown on a NANAO (Nano Corp., Matto, Japan) 21-inch grayscale data display at a frame rate of 120 Hz. The luminance of black pixels was 0.38 cd/m^2, the luminance of white pixels was 68.1 cd/m^2, and the background was 34.2 cd/m^2. A system of mirrors modified from a Helioth–Wheatstone stereoscope (31, 32) directed the left half of the screen to the left eye and the right half to the right eye, separated by a baffle, so that each eye's 144 × 144 pixel display was embedded in a larger uniform surround. The display was controlled by an 8600/200 Power PC Macintosh (Apple, Cupertino, CA) running a Matlab (Mathworks, Natick, MA) program using extensions from PSYCHTOOLBOX (33, 34).

Experiment 1: Direction-Discrimination Task. ***Observers.*** Two naïve observers and an author served in Experiment 1. Their average age was 25 years. All observers had normal or corrected-to-normal visual acuity. The naïve observers were compensated for their participation in the experiment.

Procedure. Observers were asked to fixate at the center of the screen before each trial started. The fixation image was a Nonius cross, through fusion (Fig. 1*A*), on the horopter. After observers aligned their eyes properly and fused the Nonius, the observer pressed the space bar of a keyboard to initiate a trial. Each spatial–temporal combination was repeated 40 times in pseudorandom sequence, yielding 3 (spatial frequencies) × 6 (temporal frequencies) × 40 = 720 trials in a session. The phase of the first frame was randomly varied. Observers reported perceived direction of movement (up or down) of the horizontal squarewave gratings. Feedback was given immediately after response. It took 1–1.5 h to complete a session, including initial practice and a break.

Experiment 2: Pattern Recognition Task. The observers and the moving stimuli were the same as in Experiment 1. In Experiment 2, however, observers indicated the spatial details of the moving pattern, instead of the direction of movement, by judging the perceived gratings as thin, medium, or thick corresponding to three presented spatial frequencies (0.9, 0.6, and 0.45 c/d, respectively) by pressing one of three response keys. In addition to the six temporal frequencies used in Experiment 1, counterphase flicker (8.3 or 6.3 Hz) was included. All combinations were presented in pseudorandom sequence, yielding 3 spatial frequencies × 7 temporal frequencies × 40 trials per condition = 840 trials in a session. The phase of the first frame was randomly chosen on each trial. The grating patterns were visible only when the stimuli were binocularly fused. Feedback was given immediately after each response. It took 1–1.5 h to complete a session, including breaks.

Experiment 3: Speed Rating Task. Observers were trained to apply particular speed labels to a set of six reference stimuli moving at different speeds. The moving patterns had both stereo and luminance-motion cues (so there was obvious motion), although the patterns looked indistinguishable from those in the experiment.[‡‡] The temporal frequencies of the six training stimuli were 0, 2, 4, 6, 8, and 10 Hz (all 0.6 c/d), and their assigned labels were 0, 2, 4, 6, 8, and 10, respectively. The maximum speed (10) corresponded to 16.6° per second. The zero-speed stimuli were counterphase flickering gratings at temporal frequencies of 8.3 Hz (observer CT) and 6.2 Hz (observer YT). A new stereogram occurred every 50 ms (observer CT) or 67 ms (observer YT) in all training and test stimuli. Both observers learned the labeling scheme to criterion in <1 hour.

After the training session, observers were shown the same type of stereo motion stimuli as in the previous two experiments. In Experiments 1 and 2, different spatial and temporal frequencies occurred randomly in a mixed-list design. In Experiment 3, observers were presented with three blocks of 30 stimuli. Within each block, spatial frequency was constant (0.9, 0.6, or 0.45 c/d), and the temporal frequency was chosen randomly from the set of temporal frequencies. Observers were asked to rate the speed of the stereo motion (from 0 to 10, with precision of up to two decimal places if desired) by using the speed scale established in the training session. To make the speed estimates more reliable, all six training stimuli (in random order) were displayed after every 20 trials (no response required) to remind the observers of the speed rating scale. Additionally, to evaluate the observers' consistency in using the trained scale, 20 trials of training stimuli (i.e., stimuli with depth plus luminance gratings) were inserted into the main experiment, unbeknownst to the observers.

[‡‡]The sample patterns were constructed to prevent any perception of motion standstill during the training. A squarewave luminance grating, with modulation 10 times above detection threshold, was superimposed on the experimental gratings. This compound stimulus contained information processed by the luminance-sensitive first-order motion system as well as the stereo-sensitive third-order motion system. The first-order motion system can function well at speeds of up to 16 Hz, allowing this motion system to detect motion in the range presented during training (0–10 Hz).

We thank Dr. Hyungjun Kim for assistance in programming. This research was supported by the Air Force Office of Scientific Research, Life Science Program.

1. Lu Z-L, Lesmes LA, Sperling G (1999) *Proc Natl Acad Sci USA* 96:8289–8294.
2. Lu Z-L, Lesmes LA, Sperling G (1999) *Proc Natl Acad Sci USA* 96:15374–15379.
3. Ramachandran VS, Gregory RL (1978) *Nature* 275:55–57.
4. Moreland, D (1980) in *Colour Vision Deficiencies*, ed Verriest BG (Hilger, Bristol, UK), pp 299–305.
5. Livingstone MS, Hubel DH (1987) *J Neurosci* 7:3416–3468.
6. Cavanagh P, Tyler CW, Favreau OE (1984) *J Opt Soc Am A* 1:893–899.
7. Mullen KT, Boulton JC (1992) *Vision Res* 32:483–488.
8. Teller DY, Lindsey DT (1993) *J Opt Soc Am A* 10:1324–1331.
9. Foster D (1969) *Vision Res* 9:577–590.
10. Campbell FW, Maffei L (1979) *Nature* 278:192–193.
11. Lichtenstein M (1963) *J Opt Soc Am A* 53:304–306.
12. Campbell FW, Maffei L (1981) *Vision Res* 21:713–721.
13. van Doorn AJ, Koenderink JJ, van de Grind WA (1985) *Perception* 14:209–224.
14. van de Grind WA, Koenderink JJ, van Doorn AJ (1986) *Vision Res* 26:797–810.
15. Van de Grind WA, Koenderink JJ, van Doorn AJ, Milders MV, Voerman H (1993) *Vision Res* 33:1089–1107.
16. Cohen R (1963) *Scand J Psychol* 6:257–264.
17. Schouten JF (1967) In *Models for the Perception of Speech and Visual Form*, ed Wathen-Dunn I (MIT Press, Cambridge, MA), pp 44–45.
18. MacKay D (1982) *Perception* 11:359–360.
19. Hunzelmann N, Spillmann L (1984) *Vision Res* 24:1765–1769.
20. Taylor MM (1963) *Percept Motor Skills* 16:513–519.
21. Julesz B, Payne R (1968) *Vision Res* 8:433–444.
22. Troxler D (1804) In *Ophthalmische Bibliothek II.2*, eds Himly K, Schmidt JA (Friedrich Frommann, Jena, Germany), pp 1–119.
23. Chubb C, Yellott JI (2002) *J Opt Soc Am A* 19(5):825–832.
24. Hubel DH, Wiesel TN (1962) *J Physiol (London)* 160:106–154.
25. Kowler E, Steinman R (1980) *Vision Res* 20:273–276.
26. Lu Z-L, Sperling G (1995) *Vision Res* 35:2697–2722.
27. Lu Z-L, Sperling G (2002) *J Opt Soc Am A* 19:2144–2153.
28. Lu Z-L, Sperling G (2001) *J Opt Soc Am A* 18:2331–2370.
29. Tseng CH (2004) Dissertation (University of California, Irvine, CA).
30. Lu Z-L, Sperling G (1995) *Nature* 377:237–239.
31. Wheatstone C (1838) *R Soc Lond, Philosophical Transactions*, 371–394.
32. Dudley LP (1951) *Stereoptics: An Introduction* (MacDonald, London).
33. Brainard DH (1997) *Spat Vis* 10:433–436.
34. Pelli DG (1997) *Spat Vis* 10:437–442.